

# A Class of Analytical Functions to Study the Lightning Effects Associated With the Current Front

F. Heidler, J. Cvetić

## Abstract

*The lightning currents are measured on tall structures and by artificially initiated lightning. Additionally they are deduced from the remote electric or magnetic field radiated during the so-called return stroke phase, when the lightning current is flowing to earth. For this purpose return stroke models were developed giving the dependency between the field data and the current along the ionized return stroke channel. The most frequently employed models use the so-called channel-base currents, which are commonly expressed by analytical functions to simplify the calculation procedure. A review is given about a class of analytical functions being very convenient in such calculations. The special attention is given to the type of current function most frequently used in lightning research and standardization. With these functions the fine structure in the current front can be studied, which is of basic interest with respect to the lightning protection.*

## 1 Introduction

The lightning currents are preferably studied on elevated structures due to increasing probability of the strike with the height [1]. In former lightning research they were measured with magnetic links [2] installed on various locations as power lines, masts, chimneys and high buildings (e.g. [1, 3, 4, 5, 6]). Because only the current peak proportional to the maximum magnetic field strength [2] is captured with this method, nowadays oscilloscopes are mainly employed for the recording of the current waveform. One of the first important experiments was carried out on the Empire State Building in New York City, USA [7]. Similar experiments were performed on a 60 m high mast in South Africa [8] and in Japan [9], where the currents were measured in winter thunderstorms. In Russia even captive balloons connected with ground by a steel wire [10] were used.

The majority of the currents, however, was measured on tall telecommunication towers. The well-known experiments were carried out on two 40 m high telecommunication towers in Italy [11], on a 248 m high telecommunication tower near St. Chrischona, Switzerland [12] and on a 160 m high telecommunication tower located on the mountain Peissenberg near Munich, Germany [13, 14]. The highest towers were the 540 m high Ostankino tower in Moscow, Russia [15] and the 553 m high Toronto Canadian National Tower, Canada [16]. The most important current data, however, stem from the experiments of Prof. Berger, who had been recording the lightning currents during about 30 years on a telecommunication tower situated on the mountain San Salvatore near Lugano, Switzerland ([17, 18, 19]).

Based on the current measurements and on the observation of the lightning channel two different types of

lightning to ground were identified, namely the cloud-to-ground lightning and the ground-to-cloud lightning (e.g. [7, 8, 18, 20, 21]). In the case of cloud-to-ground lightning the discharge process starts with a downward going leader from the positive or negative charge centers inside the thunder cloud [22]. In the striking point, however, the first current component is always associated with an impulse current, which may be followed by a continuing current and individual impulse currents, respectively. The cloud-to-ground lightning are characteristic for the flat country and small structures up to a height of several tens of meters.

On the other hand the ground-to-cloud lightning are typical for structures exceeding 60 m. Preferably they start from the top, when the electric field is high enough to initiate an upward going leader. In the striking point the leader is associated with a continuing current, which may be superimposed or succeeded by individual impulse currents [14]. In comparison to the cloud-to-ground lightning the impulse currents of the ground-to-cloud lightning are less severe, certainly with respect to the impulse charge, the current peak and the maximum current steepness [11]. Thus, for the protection of buildings equipped with the sensitive electrical and electronic systems, the currents of cloud-to-ground lightning have primarily to be considered.

Because the existing current data were mostly accumulated on very high structures, they were chiefly originated from ground-to-cloud lightning. Only on relatively small towers as on the two 40 m high telecommunication towers in Italy [11] and on the telecommunication tower on the Monte San Salvatore (70 m including the lightning rod) [18, 21] a higher number of cloud-to-ground lightning could be measured. Essentially based on the measurements on the Monte San Salvatore [23] the lightning parameters are fixed in various standards as in the international standard IEC

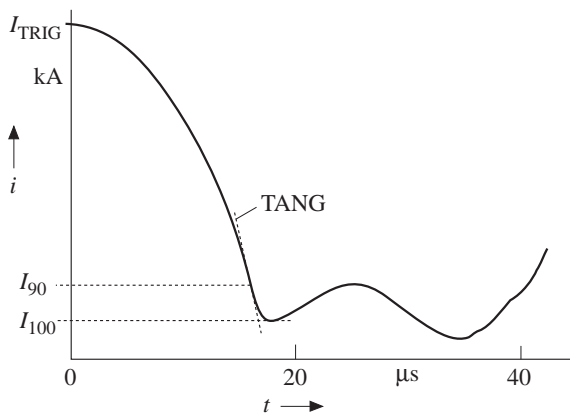


**Fig. 1.** Typical current rise of a negative cloud-to-ground lightning adopted from [23]

61312-1 [24]. The data base, however, is relatively poor and limited to about 25 positive strokes, about 100 negative first strokes and about 130 negative subsequent strokes [23]. Furthermore the front of the fast rising currents often could not be resolved sufficiently [18]. In addition it is distorted by current reflections depending on the tower height [12, 13].

Concerning the lightning protection the current front is one main subject of interest, because its high-frequency content is chiefly responsible for the coupling of over-voltages and disturbing currents into electrical circuits and electronic systems. **Fig. 1** shows the current rise proposed in [23] for negative cloud-to-ground lightning. The wave shape is concave, where the current steepness is continuously increasing up to the maximum current steepness (TANG) located at the 90%-value of the current peak. On the other hand, referring to comparable experiments in Italy [11] such a concave wave shape was only found for the first negative strokes, while the currents of the negative subsequent strokes were missing the initial slow rise portion. They were immediately starting with a fast rise resulting in a convex waveform of the current front.

In a second method the lightning were artificially triggered by rockets pulling up a metal wire from the earth toward the thundercloud. The metal wire, however, acts like a very high object, where the discharge process is initiated by an upward going leader. Similar to the ground-to-cloud lightning the first current component is given by a continuing current, which may be superimposed or succeeded by individual impulse currents [25]. Thus the triggered lightning are much more like the ground-to-cloud lightning.

Trying to avoid this shortcoming in the newest experiments of the initiated lightning the so-called altitude triggered method is used [40]. The rocket pulls up a part of the metal wire a few hundreds of meters long (not connected to the ground). The rest of the wire is made of a kevlar (insulator). The purpose of the wire is to stimulate the lightning discharge to occur and to direct it toward the ground. The lightning discharge between the lower end of the wire and the ground is considered to be more or less similar to the natural lightning.

The disadvantages of the mentioned methods could be avoided, if the lightning currents are deduced from the remote electric or magnetic field: With this method the lightning to high structures can easily be excluded and the data of a high number of cloud-to-ground lightning can be accumulated within a relatively short period of time. For this purpose different return stroke models were developed, providing the dependency between the field data and the current along the return stroke channel. From CIGRE Working Group 33.01 [26] various return stroke models were tested and finally the following models were proposed for the calculation purpose, namely the *Bruce-Golde* (BG) model [27], the transmission line model (TL) [28], the modified transmission line model (MTL) [29], the traveling current source model (TCS) [30] and the *Diendorfer-Uman* model (DU) [31].

All of these models use the so-called channel-base current, where the current in the striking point is a required model parameter, while the electric and magnetic fields are an issue of the calculation process. The direct evaluation of the current from the field data is therefore impossible except of far distant lightning, where the use of far distant field approaches simplifies the calculation algorithm. Such approaches are available for the DU-model [32], for the TCS-model [33] and for the TL-model [34]. In general, however, the current is evaluated with an iterative process, where the current waveform is varied as long as the calculated and measured fields agree sufficiently. For this application analytical current functions are preferred allowing an easy variation of the current waveform.

In conclusion, analytical current functions are needed to simplify the evaluation of the current parameters from the field data [35]. Besides they are also used in standardization [24] and in simulation models, e.g. in computer codes to calculate the voltages and currents coupled into cables and lines by lightning (e.g. [36]). As mentioned above one important source of interference is the high-frequency content of the lightning current. Concerning this requirement in the further text a review is given about a class of analytical current functions, which especially allows to model the fine structure during the current rise.

## 2 Basic features of the lightning current functions

### 2.1 Requirement of the analytical representation of the lightning current

In the calculation with the return stroke models the current as well as the current steepness and the charge are needed at each instant of time and in each point of the ionized return stroke channel [34]. For the considered return stroke models using channel-base current this requirement includes that the current  $i(t)$ , the current steepness  $di/dt$  and the charge  $Q = \int i \cdot dt$  are needed in the striking point. If the field derivatives are investigated, the second time-derivation of the current,  $d^2i/dt^2$ , is required, too. Therefore, a current function should be able to be differentiated at least twice without

any discontinuity. Especially, the first time-derivation is not allowed to have a discontinuity at the instant of time  $t = 0$  and  $(di/dt)_{t=0}$  must be equal to zero. This condition is not fulfilled in case of the double exponential current function, given by

$$i = \frac{i_{\max}}{\eta} \left( \exp\left(-\frac{t}{\tau_1}\right) - \exp\left(-\frac{t}{\tau_2}\right) \right), \quad (1)$$

with the following correction coefficient of the current peak  $i_{\max}$ :

$$\eta = \exp\left(-\frac{t_{\max}}{\tau_1}\right) - \exp\left(-\frac{t_{\max}}{\tau_2}\right), \quad (2a)$$

with

$$t_{\max} = \frac{\tau_1 \tau_2}{\tau_1 - \tau_2} \ln\left(\frac{\tau_1}{\tau_2}\right). \quad (2b)$$

Due to the discontinuity of the first time derivative at  $t = 0$ , several modifications of eq. (1) are proposed to reduce the slope of the current at this instant of time [37, 38]. The condition  $(di/dt)_{t=0} = 0$ , however, is not fulfilled by any of these functions.

The electric field of lightning can be separated into a near distant field component, an intermediate distant field component and a far distant field component. The near distant field component is determined by the charge, the intermediate distant field component by the current and the far distant field component by the current derivative [34]. Concerning lightning protection the maxima of these parameters are taken into account, namely the maximum current derivative  $(di/dt)_{\max}$ , the current peak  $i_{\max}$  and the total charge  $Q = \int i_{\max} \cdot dt$  [39]. To investigate the influences of these parameters independently a current function should allow their separate variation.

From the experimental results it can be concluded, that an analytical current function should additionally allow to vary the location of the maximum current steepness in a wide range. Even the location of  $(di/dt)_{\max}$  at the 90%-current value should be possible as proposed in [23] ( Fig. 1).

## 2.2 Deduction of the current function

In the following it is assumed that the current is starting to flow at  $t = 0$ . Before this time the current is considered to be zero:  $i = 0$ , for  $t \leq 0$ . To enable a separate variation of the total charge, the maximum current steepness and the current peak  $i_{\max}$  a rise function  $x(t)$  and a decay function  $y(t)$  are defined as follows [33, 41]:

$$i = i_{\max} \cdot x(t) \cdot y(t) \quad (3)$$

The concept considers, that the rise function  $x(t)$  determines only the current rise and the decay function  $y(t)$  only the current decay. A decoupling between the two functions is achieved, if during the current rise the decay function becomes  $y(t) \approx 1$  and if during the current decay the rise function becomes  $x(t) \approx 1$ . Because due to the lightning protection the fine structure in the decaying current is of minor interest, generally an ex-

ponential decay is taken into account. For the decay function one obtains:

$$y(t) = \exp\left(-\frac{t}{\tau}\right). \quad (4)$$

The exponential decay function fulfills the condition of the current rise:  $y(t) \approx 1$ . The fine structure in the current rise is modeled by the following class of functions [33]:

$$x(t) = \frac{f(t) + \left(\frac{t}{T}\right)^n}{g(t) + \left(\frac{t}{T}\right)^n}. \quad (5)$$

During the current decay the function  $x(t)$  is approximately equal to 1, if the exponent  $n$  is chosen high enough. The term  $(t/T)^n$  determines the change from the current rise to the current decay at the instant of time  $t \approx T$ . With the correction factor for the current peak,  $\eta$ , the expression of the current function finally follows to:

$$i(t) = \frac{i_{\max}}{\eta} \frac{f(t) + \left(\frac{t}{T}\right)^n}{g(t) + \left(\frac{t}{T}\right)^n} \cdot y(t). \quad (6)$$

Due to  $(t/T)^n = 0$  for  $t = 0$  only the ratio  $f(t)/g(t)$  determines the beginning of the current rise. A lot of various functions as trigonometric or polynomial functions can be applied successfully to  $f(t)$  and  $g(t)$ . With a relatively high exponent  $n$  a very good decoupling between the current rise and the current decay can be achieved. On the other hand a lower exponent may be advantageous to make this change smoother.

## 2.3 Application of analytical unit step function

From eq. (6) one obtains a special type of function assuming  $g(t) = 1$ . Eq. (6) becomes:

$$i(t) = \frac{i_{\max}}{\eta} \left[ \frac{f(t)}{1 + \left(\frac{t}{T}\right)^n} \cdot y(t) + \frac{\left(\frac{t}{T}\right)^n}{1 + \left(\frac{t}{T}\right)^n} \cdot y(t) \right]. \quad (7)$$

Because the first term of eq. (7) determines the current rise only, the decay function is approximated by  $y = 1$  for this term. Hence it follows [33]:

$$i(t) = \frac{i_{\max}}{\eta} [A(t) \cdot f(t) + B(t) \cdot y(t)], \quad (8a)$$

with the functions

$$A(t) = \frac{1}{1 + \left(\frac{t}{T}\right)^n}; \quad B(t) = \frac{\left(\frac{t}{T}\right)^n}{1 + \left(\frac{t}{T}\right)^n}. \quad (8b)$$

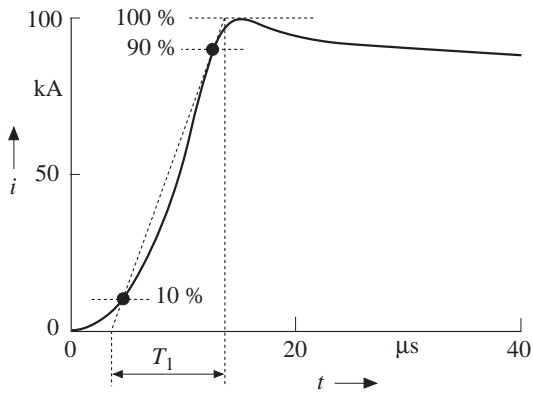


**Fig. 2.** Lightning current based on eq. (8) with the current peak  $i_{\max} = 100$  kA and the coefficients  $\eta = 0.981$ ,  $n = 10$ , and  $T = 13$   $\mu\text{s}$ . The functions are chosen to  $y = \exp(-t/\tau)$ , with  $\tau = 485$   $\mu\text{s}$  and  $f(t) = \sin^2(\omega t)$ , with  $\omega = 1.1 \cdot 10^5$  (1/s)

For a high value of the exponent  $n$  the functions  $A(t)$  and  $B(t)$  result in  $A \rightarrow 1$  and  $B \rightarrow 0$ , for  $t < T$ ; for  $t > T$  they become  $A \rightarrow 0$  and  $B \rightarrow 1$ . Therefore, they can be interpreted as analytical formulations of unit step functions switching off  $f(t)$  and switching on  $y(t)$  at the instant of time  $t = T$ . A lot of various functions can successfully be applied to  $f(t)$  and  $y(t)$ . For a smooth change from the current front to the current decay, however, both functions should have approximately the same value at the switching time  $T$ :  $f(t = T) \approx y(t = T)$ .

**Fig. 2** shows an example, where the current rise is dominated by the function  $f(t)$ , which is identical to the square of the sine function. The maximum current steepness is approximately located at the 55%-current level [33]. The front duration results in  $T_1 = 10$   $\mu\text{s}$  and the time to half a value in  $T_2 = 350$   $\mu\text{s}$ . Considering the current peak  $i_{\max} = 100$  kA this 10/350  $\mu\text{s}$ -current waveform is related to the first stroke of the standard IEC 61312-1, protection level III-IV [24].

**2.4 Application of power functions**

With regard to Fig. 1 it should be possible to vary the location of  $(di/dt)_{\max}$  between the 0%- and the 90%-current levels. For this purpose in [33, 42] the use of power functions is proposed in combination with the exponential decay function of eq. (4). With the exponents  $k_i, m_i < n$  this type of function is given by:

$$i(t) = \frac{i_{\max}}{\eta} \frac{a_1 \left(\frac{t}{T}\right)^{k_1} + a_2 \left(\frac{t}{T}\right)^{k_2} + \dots + \left(\frac{t}{T}\right)^n}{b_0 + b_1 \left(\frac{t}{T}\right)^{m_1} + b_2 \left(\frac{t}{T}\right)^{m_2} + \dots + \left(\frac{t}{T}\right)^n} \exp\left(-\frac{t}{\tau}\right). \tag{9}$$

To avoid the discontinuity at the instant of time  $t = 0$  the coefficients  $k_i, m_i$  should be greater than 1. Lightning currents with a concave current rise (Fig. 1) are achieved with the following simplification considering  $k < n$  [33, 42]:

$$i(t) = \frac{i_{\max}}{\eta} \frac{a \left(\frac{t}{T}\right)^k + \left(\frac{t}{T}\right)^n}{1 + \left(\frac{t}{T}\right)^n} \exp\left(-\frac{t}{\tau}\right). \tag{10}$$

**Fig. 3** shows two examples both representing a 10/350  $\mu\text{s}$ -current waveform analogously to Fig. 2. The initial slow rise of the concave current front is associated with a relatively low value of  $k$ . For the current of Fig. 3a the maximum current steepness is located at the 70%-current level. If the exponent  $n$  increases, the maximum current steepness also increases and is placed closer to the current peak. For the considered exponent  $n = 60$  (Fig. 3b) the maximum current steepness is located at the 90%-current level as proposed in [23] (Fig. 1).

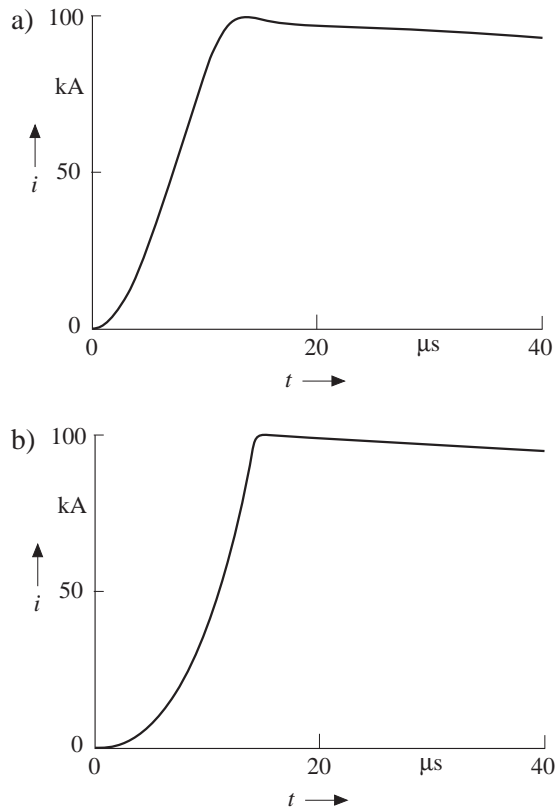


**Fig. 3.** Lightning currents based on eq. (10) with the current peak  $i_{\max} = 100$  kA. The coefficients are given by: a)  $\eta = 1.04$ ,  $a = 1$ ,  $k = 2.2$ ,  $n = 10$ ,  $T = 13$   $\mu\text{s}$ ,  $\tau = 485$   $\mu\text{s}$ ; b)  $\eta = 0.983$ ,  $a = 1$ ,  $k = 2.5$ ,  $n = 60$ ,  $T = 14$   $\mu\text{s}$ ,  $\tau = 485$   $\mu\text{s}$

**2.5 Lightning currents with two different rise portions**

In [43] it is reported, that the front of the lightning radiated fields is sometimes not increasing continuously, but in two distinct rise portions. One obtains such a field waveform considering a current showing also two rise portions [43]. This kind of current is achieved with the following adaptation of eq. (9):

$$i(t) = \frac{i_{\max}}{\eta} [X(t) + (1 - c)Y(t)] \exp\left(-\frac{t}{\tau}\right), \tag{11a}$$

with

$$Y(t) = \frac{a\left(\frac{t}{T}\right)^k + \left(\frac{t}{T}\right)^{n_1}}{1 + \left(\frac{t}{T}\right)^{n_1}}; X(t) = \frac{\left(b\frac{t}{T}\right)^{n_2}}{1 + \left(b\frac{t}{T}\right)^{n_2}}. \quad (11b)$$

**Fig. 4a** shows an example, where the current front contains two fast rise portions. In combination with the coefficients  $a$  and  $c$  they are determined by the power functions  $Y(t)$  and  $X(t)$ , where generally  $k < n_1$  should be chosen. Due to the two current rise portions the current derivative shows the first maximum  $(di/dt)_{1/\max} = 20,5 \text{ kA}/\mu\text{s}$  and the second maximum  $(di/dt)_{2/\max} = 23,6 \text{ kA}/\mu\text{s}$  (**Fig. 4b**). The time interval between them,  $t_{1-2/di} = 1,35 \mu\text{s}$ , is determined by the coefficient  $b$ .

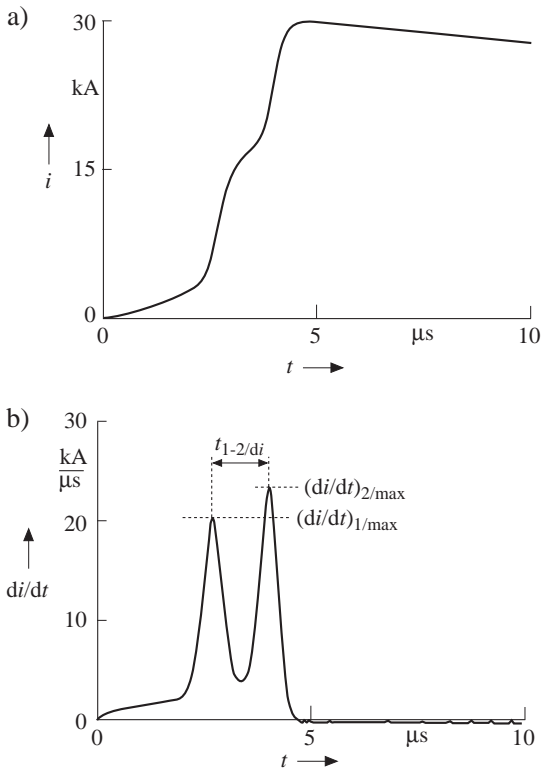


**Fig. 4.** Lightning current based on eq. (11) with the current peak  $i_{\max} = 30 \text{ kA}$  and the coefficients  $\eta = 0.937$ ,  $n_1 = 30$ ,  $k = 1.5$ ,  $n_2 = 18$ ,  $T = 4.0 \mu\text{s}$ ,  $a = 0.4$ ,  $b = 1.5$ ,  $c = 0.65$ , and  $\tau = 75 \mu\text{s}$ .

- a) Current;
- b) Current derivative

### 3. The type of power function very frequently used

#### 3.1 Characteristics of the current waveform

Concerning eq. (9) the simplest type of power function results in:

$$i = \frac{i_{\max}}{\eta} \frac{\left(\frac{t}{T}\right)^n}{1 + \left(\frac{t}{T}\right)^n} \exp\left(-\frac{t}{\tau}\right). \quad (12)$$

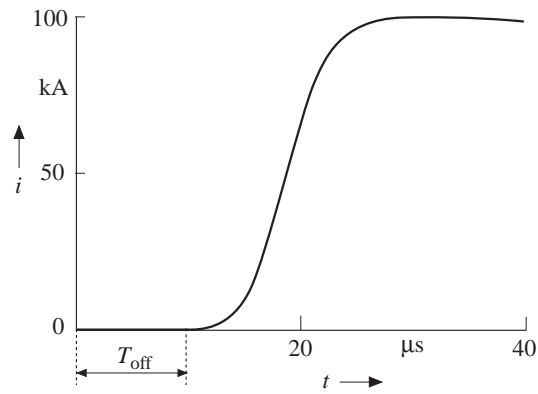


**Fig. 5.** Lightning current based on eq. (12) with the current peak  $i_{\max} = 100 \text{ kA}$  and the coefficients  $n = 10$ ,  $\eta = 0.930$ ,  $T = 19 \mu\text{s}$  and  $\tau = 485 \mu\text{s}$

This current function is very frequently used in lightning research, e.g. it is proposed by CIGRE, Working Group 33.01 [26]. In several standards as in IEC 61312-1 [24] the lightning currents are based on this function. **Fig. 5** shows an example representing the 10/350  $\mu\text{s}$ -current waveform of the first return stroke of IEC 61312-1, protection level III-IV [24]. Due to the chosen exponent  $n = 10$  and in combination with the relatively long front time coefficient,  $T = 10 \mu\text{s}$ , there is a significant current offset given by  $T_{\text{off}} \approx 10 \mu\text{s}$ , before an essential current starts to flow. In some applications as in calculations with return stroke models such a long offset time may distort the computation results. In this case the current functions described in chapter 2 are preferred modeling the concave current rises of the first strokes in a more realistic way (see Figs. 2, 3).

In comparison, **Fig. 6** shows the current front of a typical negative subsequent stroke with a front time of  $T_1 \approx 1 \mu\text{s}$  [23]. Due to this considerable shorter front time, the time offset is strongly reduced. Therefore, the currents of the negative subsequent strokes can be sufficiently modeled by eq. (12). For instance, in [35] it is reported that with this function the lightning current parameters of negative subsequent strokes could successfully be deduced from the associated field data.

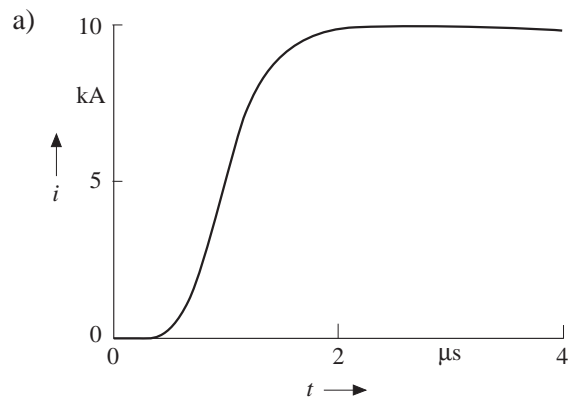


**Fig. 6.** Lightning current based on eq. (12) with  $i_{\max} = 10 \text{ kA}$  and the coefficients  $n = 5$ ,  $\eta = 0.958$ ,  $T = 1 \mu\text{s}$  and  $\tau = 75 \mu\text{s}$

### 3.2 Correction factor of the peak current

Since eq. (12) is very frequently used in standardization (e.g. see [24]) as well as in lightning research (e.g. see [26, 35]) some main features are discussed in the following. The current correction factor  $\eta$  can be found, if the instant of time  $t_{\max}$  is known, when the current attains the peak value. From the equation  $di(t_{\max})/dt = 0$  the instant of time  $t_{\max}$  can be deduced, i.e. one obtains [35]

$$\left(\frac{t_{\max}}{T}\right)^{n+1} + \frac{t_{\max}}{T} - \frac{n\tau}{T} = 0. \quad (13)$$

The analytical solution of eq. (13) cannot be given in a general case. Nevertheless the instant of time  $t_{\max}$  can be deduced from an iteration process assuming  $(t_{\max}/T)^n \gg 1$ . In this case the variation of  $t_{\max}$  has a much greater influence on the first term  $(t_{\max}/T)^{n+1}$  than on the second term  $(t_{\max}/T)$ . This behaviour allows us to use the  $(j + 1)^{\text{th}}$  iteration step of  $t_{\max}$  only for the first term, while for the second term the  $j^{\text{th}}$  iteration step is considered. From eq. (13) it follows [35]:

$$t_{\max/j+1} = T \left( \xi - \frac{t_{\max/j}}{T} \right)^{\frac{1}{n+1}}, \text{ with } \xi = \frac{n\tau}{T}. \quad (14)$$

Assuming a starting value of  $t_{\max/0} = 0$  the first approximation is given by:

$$t_{\max/1} = T \cdot \sqrt[n+1]{\xi}. \quad (15)$$

Inserting eq. (15) into eq. (14) the second approximation results in:

$$t_{\max/2} = T \cdot \sqrt[n+1]{\xi - \frac{(n+1)\sqrt[n+1]{\xi}}{T}}. \quad (16)$$

In the same way the succeeding approximations can be found leading to the following solution:

$$t_{\max} = T \cdot \sqrt[n+1]{\xi - \frac{(n+1)\sqrt[n+1]{\xi - \frac{(n+1)\sqrt[n+1]{\xi - \frac{(n+1)\sqrt[n+1]{\xi - \dots}}{T}}}{T}}}{T}}. \quad (17)$$

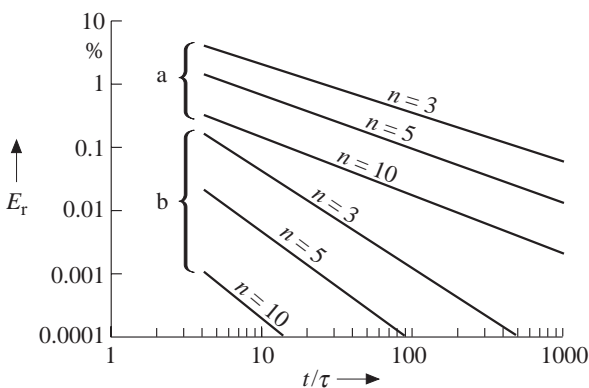


**Fig. 7.** Relative error  $E_r$  of the peak time  $t_{\max}$  in function of the quotient  $t/\tau$ . The current steepness factor  $n$  is used as a parameter.

- a) the first approximation related to eq. (15);
- b) the second approximation related to eq. (16)

**Fig. 7** shows the relative error of  $t_{\max}$ ,  $E_r$ , associated with the first and the second approximation. The accuracy increases, if the exponent  $n$  and the quotient  $\tau/T$  also increase. For the frequently accepted values of the exponent  $n \geq 3$  and the quotient  $\tau/T \geq 10$  the relative error  $E_r$  becomes below 2 % considering the first approximation of eq. (15). In case of the second approximation given by eq. (16) the relative error is much smaller, below 0.05 %. Due to this very small errors the first and the second approximations are surely accurate enough for practical applications.

### 3.3 Approximations concerning the maximum of the current steepness

The maximum of the current steepness  $(di/dt)_{\max}$  can be calculated from the equation

$$\left(\frac{d^2i}{dt^2}\right)_{t=t_1} = 0, \quad (18)$$

where  $t = t_1$  is the instant of time when the current derivative attains the maximum. Since the maximum occurs during the current rise, in the following text it is assumed  $\exp(-t/\tau) \approx 1$ , for  $t = t_1$ . Hence from eq. (12) one obtains the approximation [41, 35]

$$t_1 = T \left( \frac{n-1}{n+1} \right)^{\frac{1}{n}}. \quad (19)$$

Using eq. (19) the maximum of the current steepness is approximately given by [41, 35]

$$\left(\frac{di}{dt}\right)_{\max} = \frac{i_{\max}}{\eta} \frac{1}{T} \frac{n^2 - 1}{4n} \left( \frac{n+1}{n-1} \right)^{\frac{1}{n}}. \quad (20)$$

Concerning eq. (20) the relative error of the maximum current steepness becomes less than 1 % for the exponent  $n \geq 2$ . Substituting eq. (19) in eq. (12) one obtains the magnitude of the current when the current derivative achieves the maximum steepness [41, 35]

$$i(t = t_1) = \frac{i_{\max}}{\eta} \frac{n-1}{2n}. \quad (21)$$

From eq. (21) it follows that the maximum current steepness can be varied between the 0 %- and the 50 %-current level. The 50 %-current level results for an infinite exponent  $n$ :  $n \rightarrow \infty$ .

## 4 Lightning current defined in the international standard IEC 61312-1

### 4.1 Current parameters fixed in IEC 61312-1

The general principles of the protection against the lightning current and the associated field are given in the international standard IEC 61312-1 [24]. Meanwhile the current features fixed there are accepted by

several standards as the German military standard VG 95371-10 [44]. Based on the results of CIGRE reported in [23, 45] the current parameters are classified in four protection levels according to different probabilities of occurrence. The current waveform is fixed by eq. (12) choosing an exponent of  $n = 10$ , i.e. one obtains:

$$i = \frac{i_{\max}}{\eta} \frac{\left(\frac{t}{T}\right)^{10}}{1 + \left(\frac{t}{T}\right)^{10}} \exp\left(-\frac{t}{\tau}\right). \quad (22)$$

Referring to eq. (21) the maximum current steepness is approximately located at the 45 %-current level. The coefficients of eq. (22) are given in **Tab. 1** distinguishing between the first (positive or negative) stroke and the negative subsequent stroke. For the first stroke the front duration ( $T_1$ ) and the time to half value ( $T_2$ ) result in  $T_1 = 10 \mu\text{s}$  and  $T_2 = 350 \mu\text{s}$  and for the negative subsequent stroke in  $T_1 = 0.25 \mu\text{s}$  and  $T_2 = 100 \mu\text{s}$ . The associated current rises are shown in Fig. 5 for the first stroke and in Fig. 8 for the negative subsequent stroke, respectively.

Parameter	Symbol	Value for first stroke	Value for subsequent stroke
front time coefficient	$T$	19.0 $\mu\text{s}$	0.454 $\mu\text{s}$
decay time coefficient	$\tau$	485 $\mu\text{s}$	143 $\mu\text{s}$
correction coefficient	$\eta$	0.930	0.993

**Tab. 1.** Coefficients of eq. (22) according to IEC 61312-1 [24]

**Tab. 2** contains the values of the current peak for the different protection levels fixed in IEC 61312-1 [24]. For the subsequent stroke of protection level I one obtains the highest value of the maximum current derivative resulting in  $(di/dt)_{\max} \approx 280 \text{ kA}/\mu\text{s}$ . This value is approximately associated with the 1 %-probability of occurrence [23].

Protection level	Symbol	First stroke	Subsequent stroke
I	$i_{\max}$	200 kA	50
II	$i_{\max}$	150 kA	37.5
III-IV	$i_{\max}$	100 kA	25

**Tab. 2.** Current peak according to IEC 61312-1 [24]

In comparison, with unaltered values of the front duration,  $T_1 = 0.25 \mu\text{s}$ , and the current peak,  $i_{\max} = 50 \text{ kA}$ , the maximum current steepness of  $(di/dt)_{\max} = 545 \text{ kA}/\mu\text{s}$  would result, if the double exponential current waveform of eq. (1) is considered. This unrealistic high current steepness makes clear, that the double exponential current function of eq. (1) represents a very rough approximation with respect to the front of lightning currents.

## 4.2 Frequency domain approach

Hitherto in literature no analytical solution of the standardized current function of eq. (22) has been known in the frequency domain. Therefore, the following two approximations are given, which are normally sufficient for practical application.

Based on the Fourier's transform (see chapter 6) the following frequency domain formula gives the first approximation [42]:

$$\underline{F}(j\omega) = \frac{i_{\max}}{\eta} \underline{A}(j\omega) \cdot \exp\left(-T\left(\frac{1}{\tau} + j\omega\right)\right), \quad (23a)$$

with

$$\underline{A}(j\omega) = \frac{1}{\frac{1}{\tau} + j\omega} \cdot \frac{1}{\left(1 + \left(\frac{\omega T}{20}\right)^2\right)^5}. \quad (23b)$$

The accuracy of the approximation is tested by converting numerically the frequency domain solution into the time domain. Then the resulting curve is compared with the current waveform given by eq. (22). **Fig. 8** shows the comparison concerning the subsequent stroke of IEC 61312-1, protection level III-IV. For both the first and the subsequent strokes of this standard only very small deviations were found of the order of 1 %, except in the region of the current peak, where the deviation increases up to about 5 %.

The accuracy nearby the maximum is increased with the following correction function [42]:

$$\underline{B}(j\omega) = \frac{0.07}{\frac{4.2}{T} + j\omega} \cdot \frac{\exp\left(-\frac{j\omega t}{9}\right)}{\left(1 + \left(\frac{\omega T}{50}\right)^2\right)^5}. \quad (24)$$

Eq. (23a) is modified as follows:

$$\underline{F}(j\omega) = \frac{i_{\max}}{\eta} (\underline{A}(j\omega) - \underline{B}(j\omega)) \cdot \exp\left(-T\left(\frac{1}{\tau} + j\omega\right)\right). \quad (25)$$

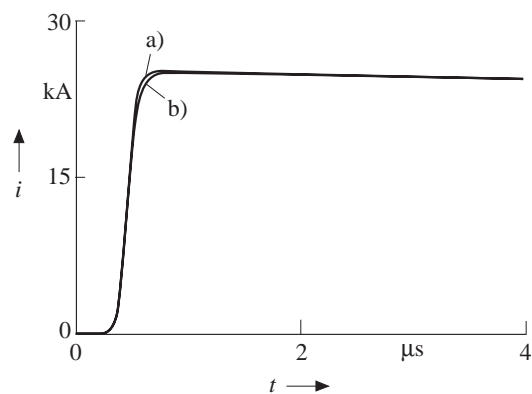


**Fig. 8.** Front of the subsequent stroke current of IEC 61312-1, protection level III-IV [24].  
a) Current of eq. (22);  
b) Inverse Fourier's transform of eq. (23)

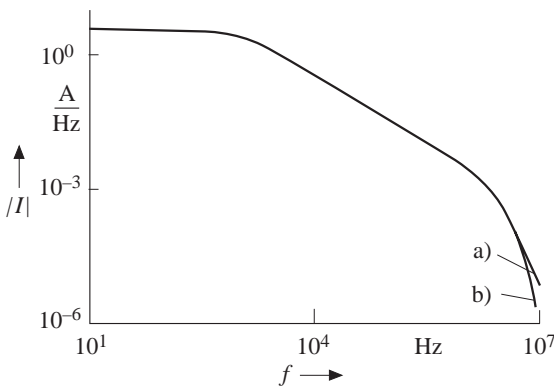


**Fig. 9.** Amplitude density spectrum of the subsequent stroke current of IEC 61312-1, protection level III-IV [24]. a) Numerical Fourier's transform of eq. (22); b) Approximation due to eq. (25)

Concerning eq. (25) the maximum of the relative error is reduced to about 1 % also nearby the current maximum.

**Fig. 9** shows the comparison in the frequency domain considering again the subsequent stroke of IEC 61312-1, protection level III-IV [24]. The spectrum of the approximation (curve b) is nearly identical to the spectrum resulting from the Fourier's transform of eq. (22) (curve a). Greater deviations occur only outside the first six decades of the spectrum amplitudes.

### 5 Summary

The coupling of voltages and currents into electrical systems is mainly caused by the high-frequency content of the lightning current and the associated electric and magnetic field. One main subject concerning lightning protection is therefore the analysis of the current front. The most important parameters of interest are the current peak, the maximum current derivative and its location in the current waveform. The presented class of current functions allows to vary these parameters without significant influence on the current decay. It is possible to reproduce the concave wave shape known from the currents of the first positive and negative strokes as well as the fast rising currents of negative subsequent strokes.

The type of current function most frequently used in lightning research and standardization is analyzed more in detail. The analysis includes the approximations related to the current peak and the maximum of the current steepness. Finally, for the standardized function of lightning current a frequency domain approach is given, which is useful with respect to practical applications.

### 6 Appendix

A time domain function  $f(t)$  is transferred to the frequency domain by Fourier's transform. With  $j = \sqrt{-1}$  the complex spectrum  $\underline{F}(j\omega)$  is given by:

$$\underline{F}(j\omega) = \int_{-\infty}^{\infty} f(t) \cdot \exp(-j\omega t) \cdot dt.$$

Inverse Fourier's transform is given by

$$f(t) = \frac{1}{2\pi} \int_{-\infty}^{\infty} \underline{F}(j\omega) \cdot \exp(+j\omega t) \cdot d\omega.$$

### 7 List of symbols

$j$	$\sqrt{-1}$
$\xi$	dimensionless parameter
$\omega = 2 \pi f$	circle frequency
$a, b, c$	coefficients of the current functions
$k, m, n$	exponents
$x(t), y(t)$	functions for the current rise and decay
$X(t), Y(t)$	auxiliary functions of the current
$f(t), g(t)$	time domain functions
$\underline{F}(j\omega)$	frequency domain function
$A(t), B(t)$	auxiliary functions in the time domain
$\underline{A}(j\omega), \underline{B}(j\omega)$	correction functions in the frequency domain
$E_r$	relative error
$t$	time
$t_{\max}$	time of the current peak
$t_1$	time of the maximum current steepness
$\tau, \tau_1, \tau_2$	time coefficient of an exponential function
$T$	front time coefficient
$T_1$	front duration
$T_2$	time to half value
$T_{\text{off}}$	time offset
$i$	current
$i_{\max}$	current peak
$\eta$	correction coefficient of the current peak

### References

- [1] *Popolansky, F.*: Lightning current measurement on high objects in Czechoslovakia. 20<sup>th</sup> Int. Conf. on Lightning Protection (ICLP), Interlaken/Switzerland 1990, Proc. report 1.3
- [2] *Grünwald, H.*: Die Messung von Blitzstromstärken an Blitzableitern und Freileitungsmasten. etz (1934), no. 21, pp. 505–509
- [3] *Miladowska, K.*: Vergleichung der Blitzresultate von hohen Schornsteinen und den Zählern. 14<sup>th</sup> Int. Conf. on Lightning Protection (ICLP), Gdansk/Poland 1978, Proc. report R-1.04
- [4] *Kulikow, D.*: Blitzströme. 14<sup>th</sup> Int. Conf. on Lightning Protection (ICLP), Gdansk/Poland 1978, Proc. report R-1.05
- [5] *Grünwald, H.*: Die Messung von Blitzstromstärken an Blitzableitern und Freileitungsmasten. etz (1934), no. 22, pp. 536–539
- [6] *Zaduk, H.*: Neuere Ergebnisse der Blitzstromstärkemessungen an Hochspannungsleitungen. etz (1935), no. 17, pp. 475–479
- [7] *McEachron, K.B.*: Lightning to the Empire State Building. J. of the Franklin Institute, vol. 227, (1939) no. 2, pp. 149–217

- [8] *Geldenhuis, H.; Eriksson, A.; Bouon, A.*: Fifteen years' data of lightning current measurement on a 60 m mast. 19<sup>th</sup> Int. Conf. on Lightning Protection (ICLP), Graz/Austria 1988, Proc. report R-1.7
- [9] *Miyake, K.; Suzuki, T.; Shinjou, K.*: Characteristics of winter lightning currents on Japan sea coast. IEEE Trans. on Power Delivery, vol. 7, (1992) no. 3, pp. 1450–1456
- [10] *Brechow, W.; Laronow, W.*: Charakteristiken des Blitzes bei Einschlägen in hohe Objekte. 16<sup>th</sup> Int. Conf. on Lightning Protection (ICLP), Budapest/Hungary 1981, Proc. report R-1.08
- [11] *Garbagnati, E.; Marioni, F.; LoPiparo, G.*: Parameters of lightning currents. Interpretation of the results obtained in Italy. 16<sup>th</sup> Int. Conf. on Lightning Protection (ICLP), Budapest/Hungary 1981, Proc. report R-1.03
- [12] *Montandon, E.; Beyerler, B.*: The lightning measuring equipment on the Swiss PTT telecommunication tower at St. Chrischona, Switzerland. 22<sup>nd</sup> Int. Conf. on Lightning Protection (ICLP), Budapest/Hungary 1994, Proc. report R-1c-06
- [13] *Zundl, T.*: Koordinierte Messungen von Blitzströmen und ihrer elektromagnetischen Felder an einem Fernmeldeturm. Phil. Thesis, Univ. of the Fed. Armed Forces, Munich/Germany, 1996
- [14] *Fuchs, F.; Landers, E.; Schmid, R.; Wiesinger, J.*: Lightning current and magnetic field parameters caused by lightning strikes to tall structures relating to interference electronic systems. IEEE Trans. on EMC, vol. 40, (1998) no. 4, pp. 444–451
- [15] *Gorin, B.N.; Lewitow, W.I.; Schkiljew, A.W.*: Einige Ergebnisse der Blitzstationenaufnahmen auf dem Ostankino-Fernsehturm. 13<sup>th</sup> Int. Conf. on Lightning Protection (ICLP), Milano/Italy 1976, Proc. report R-1.9
- [16] *Janischewskyi, W.; Hussein, A.M.; Shostak, V.; Rusan, I.; Li, J.-X.; Chang, J.-S.*: Statistics of lightning strikes to the Toronto Canadian National Tower (1978–1995). IEEE/PES Summer meeting, Denver, Colorado/U.S.A. 1996, Proc. report SM 422-6 PWRD
- [17] *Berger, K.; Vogelsang, E.*: Messungen und Resultate der Blitzforschung der Jahre 1955 bis 1963 auf dem Monte San Salvatore. Bull. SEV, vol. 56, (1965) no. 1, pp. 2–22
- [18] *Berger, K.*: Novel observations on lightning discharges: Results of research on Mount San Salvatore. Journal of the Franklin Institute, vol. 283, (1967) no. 6, pp. 478–525
- [19] *Berger, K.*: Methoden und Resultate der Blitzforschung auf dem Monte San Salvatore bei Lugano in den Jahren 1963–1971. Bull. SEV, vol. 87, (1972) no. 24, pp. 1403–1422
- [20] *Gorin, B.N.; Lewitow, W.I.; Schkiljew, A.W.*: Besonderheiten der Blitzeinschläge in den Ostankino-Fernsehturm. 13<sup>th</sup> Int. Conf. on Lightning Protection (ICLP), Milano/Italy 1976, Proc. report R-1.10
- [21] *Berger, K.*: Blitzstrom-Parameter von Aufwärtsblitzen. Bull. SEV, vol. 69, (1978) no. 8, pp. 353–360
- [22] *Schonland, B.F.J.*: The lightning discharge. Handbuch der Physik, vol. 22, (1956) pp. 576–628, Springer-Verlag, Berlin/Germany, 1956
- [23] *Anderson, R.B.; Eriksson, A.J.*: Lightning parameters for engineering application. Electra, vol. 69, (1980) pp. 65–102
- [24] IEC 61312-1, 2/95: Protection against lightning electromagnetic impulse, Part 1: General principles
- [25] *Hubert, P.; Laroche, P.; Eybert-Berand, A.; Barret, L.*: Triggered lightning in New Mexico. J. of Geophys. Res., vol. 89, (1984) no. D4, pp. 2511–2521
- [26] *Nucci, C.A.*: Lightning-induced voltages on overhead power lines. Part I: Return stroke models with specified channel-base for the evaluation of the return stroke electromagnetic field. Electra, vol. 161, (1995) pp. 74–102.
- [27] *Bruce, C.E.; Golde, R.H.*: The lightning discharge. J. IEE, London, vol. 88, (1941) part II, no. 6, pp. 487–524
- [28] *Uman, M.A.; McLain, D.K.*: Magnetic field of lightning return stroke. J. of Geophys. Res., vol. 74, (1969) no. 28, pp. 6899–6910
- [29] *Nucci, C.; Rachidi, F.*: Experimental validation of a modification of the transmission line model for LEMP calculations. 8<sup>th</sup> Int. Zurich Sympos. on EMC, Zurich/Switzerland 1989, Proc. pp. 389–394
- [30] *Heidler, F.*: Travelling current source model for LEMP calculation. 6<sup>th</sup> Int. Zurich Sympos. on EMC, Zurich/Switzerland 1985, Proc. pp. 157–162
- [31] *Diendorfer, G.; Uman, M.A.*: An improved return stroke model with specified channel-base current. J. of Geophys. Res., vol. 95, (1990) no. D9, pp. 13621–13644
- [32] *Rachidi, F.; Thottappillil, R.*: Determination of lightning currents from far electromagnetic fields. J. of Geophys. Res., vol. 98, (1993) no. D10, pp. 18315–18321
- [33] *Heidler, F.; Hopf, Ch.*: LEMP calculation and lightning current function. 8<sup>th</sup> Int. Sympos. on High Voltage Engineering (ISH), Yokohama/Japan 1993, vol. 4, Proc. pp. 273–240
- [34] *Uman, M.A.; McLain, D.K.; Krider, E.P.*: The electromagnetic radiation from a finite antenna. Amer. J. of Physics, vol. 43, (1975) pp. 33–38
- [35] *Heidler, F.; Cvetić, J.; Stanić, B.V.*: Calculation of lightning current parameters. IEEE Trans. on Power Delivery, vol. 14, (1999) no. 02, pp. 399–404
- [36] *Nucci, C.A.*: Lightning-induced voltages on overhead power lines. Part II: Coupling models for the evaluation of the induced Voltages. Electra, vol. 162, (1995) pp. 121–145
- [37] *Rajicic, D.*: Beeinflussung einer Darstellungsweise der atmosphärischen Entladung auf den maximalen Spannungswerten in den einzelnen Punkten der einfacheren Blitzschutzinstallationen. 12<sup>th</sup> Int. Conf. on Lightning Protection (ICLP), Portoroz/Yugoslavia 1973, Proc. report R. 2-12
- [38] *Gardner, R.L.; Baker, L.; Baum, C. E.; Andersh; D.J.*: Comparison of lightning with public domain HEMP waveforms on the surface of an aircraft. 6<sup>th</sup> Int. Sympos. on EMC, Zurich/Switzerland 1985, Proc. pp. 175–180
- [39] *Hasse, P.; Wiesinger, J.*: Handbuch für Blitzschutz und Erdung. 4<sup>th</sup> ed., Pflaum Verlag, Munich/Germany, 1993
- [40] *Rakov, V.A.; Uman, M.A.; Rambo, K.J.; Fernandez, M.I.; Fisher, R.J.; Schnetzer, G.H.; Thottappillil, R.; Eyberd-Berard, A.; Berlandis, J.P.; Lalonde, P.; Bonamy, A.; Laroche, P.; Bondiou-Clergerie, A.*: New Insights into lightning processes gained from triggered-lightning experiments in Florida and Alabama. J. of Geophys. Res., vol. 103, (1998) no. D12, pp. 14117–14130
- [41] *Heidler, F.*: Analytische Blitzstromfunktion zur LEMP-Berechnung. 18<sup>th</sup> Int. Conf. on Lightning Protection (ICLP), Munich/Germany 1985, Proc. pp. 63–66
- [42] *Heidler, F.; Hopf, Ch.*: Lightning current function for LEMP calculation. 22<sup>nd</sup> Int. Conf. on Lightning Protection (ICLP), Budapest/Hungary 1994, Proc. report R. 4-06
- [43] *Heidler, F.; Hopf, Ch.*: Initial and subsidiary peak of the lightning electromagnetic fields considering channel-base current and reflections at the return stroke channel. 9<sup>th</sup> Int. Sympos. on High Voltage Engineering (ISH), Graz/Austria (1995), Proc. report 6743
- [44] VG 95371-10: Elektromagnetische Verträglichkeit (EMV) einschließlich Schutz gegen den Elektromagnetischen Impuls (EMP) und Blitz. Allgemeine Grund-

lagen – Teil 10: Bedrohungsdaten für den NEMP und Blitz. Military standard

[45] Berger, K.; Anderson, R.B.; Kröniger, H.: Parameters of lightning flashes. *Electra*, vol. 41, (1975) pp. 23–37

*Manuscript received on March 21, 2000*

### The authors



**Fridolin H. Heidler** was born in Giengen, Baden-Wuerttemberg/Germany, in 1955. After the studies of Electrical Engineering at the Technical University of Munich/Germany in 1982 he joined the University of the Federal Armed Forces Munich, where he is still working. In 1987 he received his Ph.D. thesis and in 1999 the post-doctoral lecturing qualification at the Faculty of Electrical Engineering of

this University. His special interests are field calculations in the frequency and the time domain as well as the measurement of the electric and magnetic fields radiated by lightning. (University of the Federal Armed Forces Munich, Faculty of Electrical Engineering, ET 7, Werner-Heisenberg-Weg 39, D-85577 Neubiberg/Germany, Phone: +49-89-6004-3736, Fax: +49-89-6004-3723, E-mail: Fridolin.Heidler@unibw-muenchen.de)



**Jovan M. Cvetic** was born in Kotor, Montenegro/Yugoslavia, in 1962. He studied Electrical Engineering at the University of Belgrade graduating with a B.Sc. in 1988 and an M.Sc. in 1993. In 1998 he received his Ph.D. thesis at the Faculty of Electrical Engineering, University of Belgrade. He is the author or co-author of more than 20 scientific papers in journals and at the international conferences. His

main research interests are lightning return stroke modelling and LEMP interference. (Faculty of Electrical Engineering, University of Belgrade, Bulevar revolucije 73, P.O. Box 35-54, 11000 Belgrade/Yugoslavia, Phone: +381 11 3370 156, Fax: +381 11 324 8681), E-mail: cvetic\_j@kiklop.etf.bg.ac.yu)